

Effects of Differential Tectonic Uplift on Steepness and Concavity Indices and Erosion Rates in Between the Major Thrusts in Bhagirathi-Alaknanda Catchments, NW Himalayas, India



Sumit Das  and Satish J. Sangode

Abstract Geomorphology of the Bhagirathi-Alaknanda catchments draining across the northwest Himalayas was studied to understand the role of differential tectonic uplifts over landscape erosional rates and landscape shaping. We plotted longitudinal profiles of Bhagirathi and Alaknanda and identified the major thrust zones along these trunk streams. For the comprehension of differential uplift, steepness and concavity indices were computed in between major thrusts along the longitudinal profiles. The regions experiencing very high erosion were recognized through anomalously high normalized steepness index (k_{sn}) and dense distribution of knick-points on the drainage network. Further estimation of average erosion and deposition rates between the major thrusts was done through establishing linear correlation of average normalized steepness index and readily available in-situ ^{10}Be cosmogenic dating-derived erosion rate data. Our results indicated a very high erosion rate (2.87 mm/yr) between Main Central Thrust I and II (Vaikrita Thrust), related to intense uplift, high recurrence of landslides and profound fluvial incision. Regions from MBT to further south towards Ganga plain showed strong aggradation at an average rate of 3.03 mm/yr.

Keywords Tectonic uplift · Steepness index · Erosion rate · Longitudinal profile · Alaknanda · Himalayas

1 Introduction

The mighty Himalayas politically shares a considerable area of north India, Nepal, and Bhutan and forms an arc-shaped series of high mountains, showing the highest peak (Mount Everest—8848.86 m a.s.l.) of the world and several peaks that have elevation above 7000 m above sea level [a.s.l.] (e.g. Kanchenjunga, Nanga Parbat, Nanda Devi, Makalu etc.) (Fig. 1). A large number of geological-geomorphic

S. Das (✉)

Department of Geography, Savitribai Phule Pune University, Pune 411007, India

S. J. Sangode

Department of Geology, Savitribai Phule Pune University, Pune 411007, India

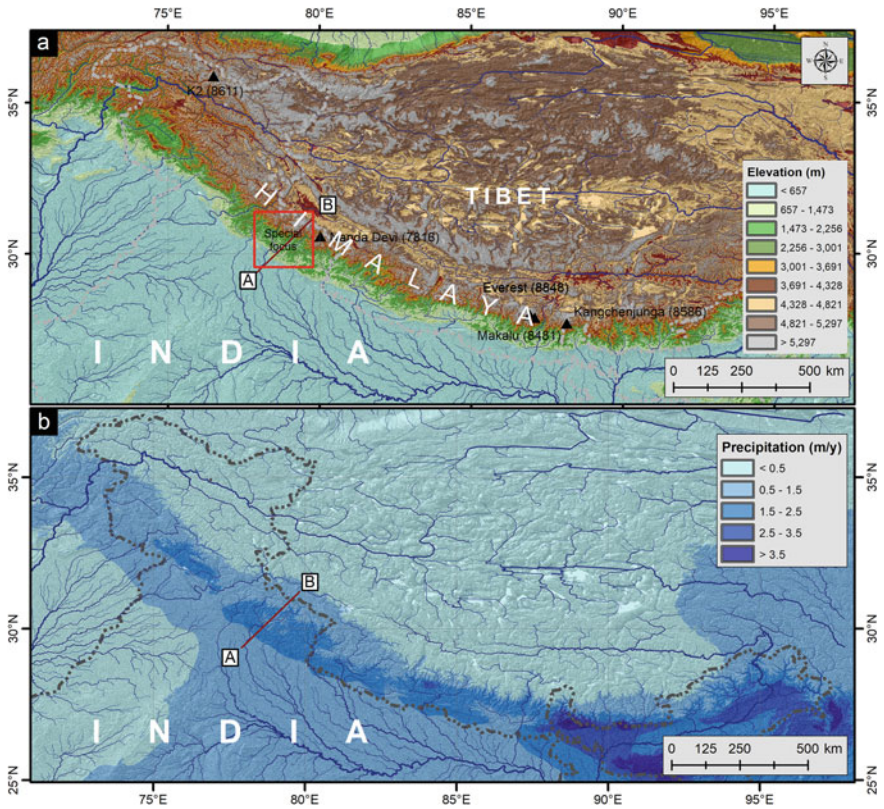


Fig. 1 **a** DEM is showing variation in elevation along the Himalayas and surrounding regions with major drainage networks. **b** Spatial distribution of rainfall along the Himalayas (*Source* <https://www.worldclim.org/>)

processes (both endogenetic and exogenetic) led to shape and reshape the landscape of the Himalayas, what we see presently. Created by continent–continent collision, the Himalayas is one of the best classic examples of the orogenic system (Dewey and Bruke 1973). To understand the geomorphic processes and diversity in the Himalayas, it is essential to look back in time and understand the continental framework that led to the rise of such massive and spectacular high ranges.

About 180 Ma ago, the Indian continent started breaking from the Gondwana land and drifted northwards at rates varying from ~4 to 20 cm/yr (Seeber et al. 1981; Patriat and Achache 1984; Pichon et al. 1992). The relatively fast, inexorable drift of the South Asian continent then nearly 50 Ma ago collided with the Eurasian plate and resulted in uplifting of huge compressed seafloor (the Tethys) and formation of an extraordinary gigantic range of fold mountains named the Himalayas that stands

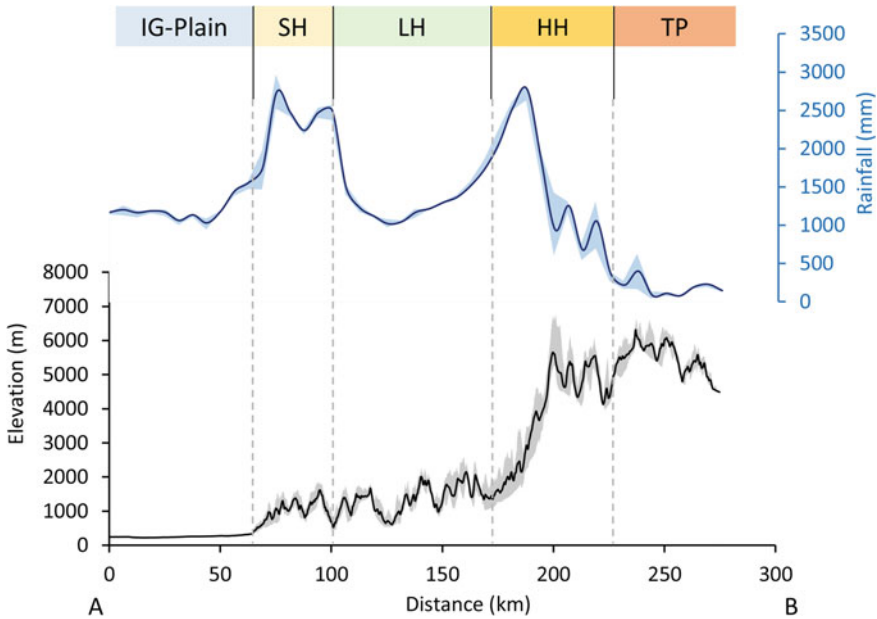


Fig. 2 Generalized broad physiographic divisions and variation in precipitation in the Himalayas (Alaknanda catchment) from south (a) to north (b). See Fig. 1. For the swath line. IG: Indo-Gangetic plain, SH: Sub-Himalayas, LH: Lesser Himalayas, HH: Higher Himalayas, TP: Tibetan Plateau

above all other places in the world (Patriat and Achache 1984). The abundant distribution of fossils of ancient sea creatures, for example, ammonites on the Himalayan sedimentary rocks indicates that the region once was beneath the ocean.

Based on the range's orientation and structure, the Himalayas can be divided into four major broad physiographic divisions (Fig. 2). The southern section comprises an Indo-Gangetic plain made of alluvium brought by the Himalayan Rivers (Singh et al. 2015). The low, frontal sub-Himalayas form the foothill region. These foothills have an average height of about 900–1500 m (Whitehouse 1990). North of the sub-Himalayas, the hill ranges within the lesser Himalayas show elevation between 700 and 2500 m. The higher Himalayas forms the highest relative relief (~6000 m) with several peaks above 8000 m. The Tibetan marginal range forms a 6000–7000 m high Tibetan plateau north of the higher Himalayas.

The Indian Summer Monsoon (ISM) modulates the process of erosion and its rates along the southern margin of the Himalayan topographic front (Bookhagen and Burbank 2006). The rainy season in the Himalayas starts from early June and continues till September; therefore, this orographic rainfall has a significant role in the erosional mechanism (Fasullo and Webster 2003). The topographic and rainfall distribution was poorly understood until the work of Bookhagen and Burbank (2006). They showed the relationship between rainfall and topographic (elevation) distribution across the Himalayas through a number of swath profiles. The monsoons, while

moving northward, experience the first significant topographic barrier due to the Lesser Himalayas, where intense orographic rainfall occurs. Once the cloud crosses Lesser Himalayas, rainfall intensity becomes less until it once again reaches the Higher Himalayas and the second phase of rainfall occurs in front of this massive topographic front. The Higher and Tethyan Himalayas receives the majority of its precipitation from the Western Disturbances responsible for the winter snow accumulation (Rees and Collins 2006; Dimri et al. 2015).

Landscapes of the Himalayas are mainly formed by the collision of continental blocks that uplifted the landmass; and the intense and variable summer monsoon precipitation shaped the modern topography in Lesser and Outer Himalayas (Abrahami et al. 2016; Sinha and Sinha 2016). The Himalayas has become a natural laboratory to understand the complex relationship between tectonic uplift and climate on erosion for the past several decades. While a large number of studies only focus on the role of uplift (e.g. Kothyari and Luirei 2016; Bhakuni et al. 2017; Sharma et al. 2018), several studies indicate a combination of climate and tectonics to play a crucial role in differential erosion rates (e.g. Vence et al. 2003; Thide et al. 2005) through geological time. Since the antecedent river response is simultaneous to both tectonic and climatic variability across the cross-sections of the Himalayas, they are ideal locales for detailed studies.

Bhagirathi and Alaknanda are two major rivers that flow across the Himalayas covering the major section of Lesser and Outer Himalayas and forming the mega river Ganga in the foothills. In the past few decades, these two rivers and the areas within the catchment have become the interests of geomorphologists to understand the complex geomorphic processes (e.g. Valdiya 1988; Tyagi et al. 2009; Ray and Srivastava 2010; Rana et al. 2016). The geomorphic processes in this region are genetically related to structural and tectonic complexities within Kumaun Lesser Himalayas as described in classical literature (Valdiya 1988). Nonetheless, the influence of climate in the formation of river terraces and stratigraphic development is very well described (e.g., Ray and Srivastava 2010). Rana et al. (2016) earlier elaborated the significance of tectonic geomorphology within the Alaknanda valley through morphometric analysis. Tyagi et al. (2009) made a remarkable discussion by identifying of differentially uplifted areas using the steepness index of the Alaknanda River profile. These workers (Tyagi et al. 2009) divided the longitudinal profiles into several reaches to compute the normalized steepness index (k_{sn}). Although considering a single longitudinal profile merely provides some instances of differential uplift and erosion at local scale, for the regional tectonic framework, it is essential to estimate k_{sn} for all the available drainages as well, and correlate the average k_{sn} with erosion rate for a robust conclusion. Therefore, the aim of this present study is set to understand the role of tectonics in the formation of anomalies on the longitudinal profiles, variation in steepness and concavity index and estimation of erosion rates in between major Himalayan thrust belts in the Alaknanda-Bhagirathi catchment. In the event of an emerging climate change scenarios marked by heavy rainfall, cloud burst triggered flash-floods or the Glacial Lake Outburst Floods (GLOF), an assessment of the longitudinal profiles across these Himalayan states is essential to anticipate their response.

2 Study Area

2.1 Location

The Alaknanda and Bhagirathi Rivers (Fig. 3) flow over the active orogeny of the Himalayas (Ray and Srivastava 2010). These two rivers cross the Himalayan thrust belts in the northern section while the southern section is characterized by the vast Ganga plain (Singh et al. 2007, 2015). River Alaknanda originates from the Satopanth glacier at an elevation of 3641 m, and the Bhagirathi originates from the Gangotri glacier near Gaumukh at an elevation of 3892 m a.s.l. These two rivers meet near Devprayag and form the sacred river Ganga. Geomorphological breaks that are marked by a series of knick points in Bhagirathi and Alaknanda show deep incision and gorges in the upper and middle reaches. Geomorphologically, these two rivers show three distinct reaches: (a) the glaciated, semi-arid U-shaped valley in the upper section; (b) steep V-shaped deep gorges in the middle reach and this section forms the main orographic barrier of the ISM and shows intense precipitation marked by numerous geomorphic processes (Bookhagen and Burbank 2006; Wasson et al. 2008); and (c) gentle slope with sediment-filled wide valley in the lower reaches.

2.2 Geology

The Alaknanda-Bhagirathi catchment shows two major geomorphic divisions: (i) the Himalayan active terrain and (ii) the Ganga foreland plain (Ray and Srivastava 2010). Himalayan thrust belt, located in the northern section of Alaknanda- Bhagirathi catchment shows several parallel thrusts marked by distinct lithology groups. The major lithology in this catchment from north to south are (i) Tethyan sedimentary, (ii) upper higher Himalayan crystalline (Vaikrita group), (iii) lower higher Himalayan crystalline (Munsiari formation), (iv) inner lesser Himalayan sedimentary, (v) outer lesser Himalayan sedimentary, and (vi) Quaternary sediment. While flowing over the Himalayas, Alaknanda river crosses the South Tibetan Detachment (STD) in the northernmost region of catchment, followed by Main Central Thrust (MCT) II and I, Main Boundary Thrust (MBT), and Main Frontal Thrust (MFT) in the south before reaching the vast Gangetic Plain.

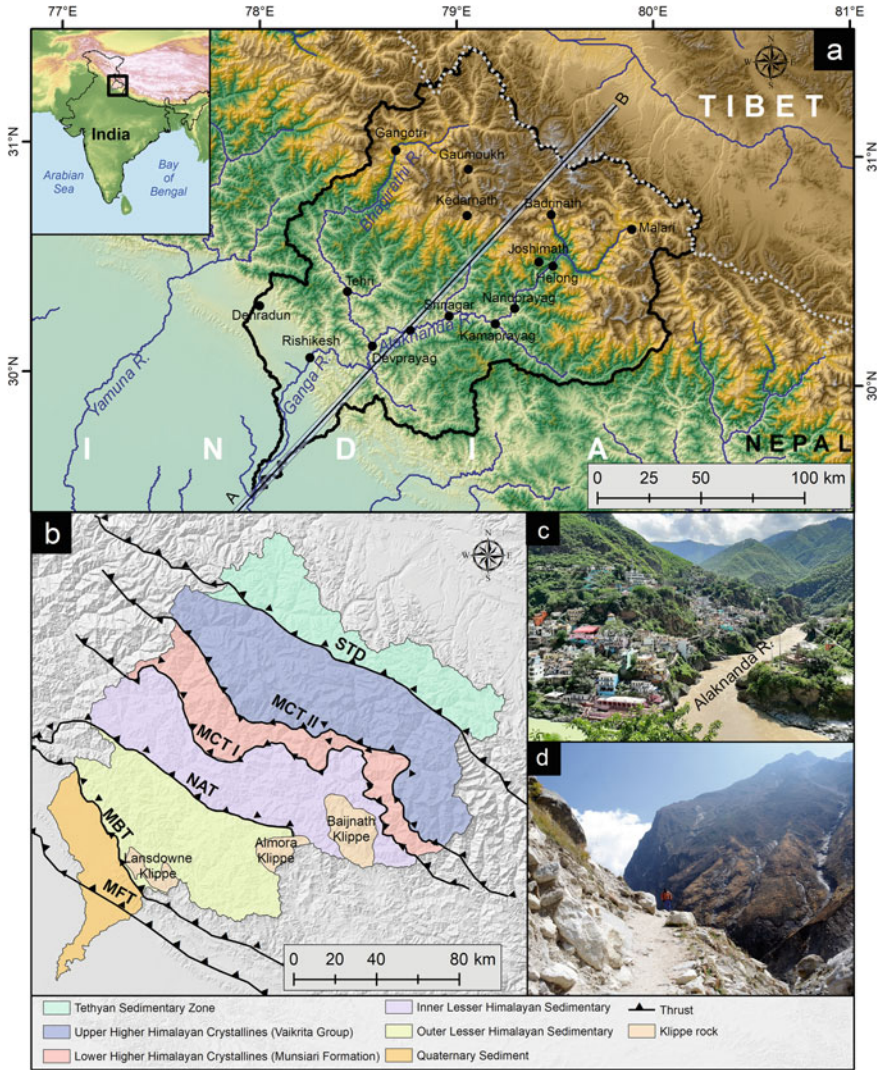


Fig. 3 Location of the Alaknanda-Bhagirathi catchment. **a** Major rivers and locations in the study area. See Fig. 2 for the swath profile of A-B. **b** Simplified geological map of the study area (reproduced after Singh 2018). Note that the thrusts are not limited as shown in this figure but continuous features along the Himalayas from west to east. **c** The confluence of Alaknanda and Bhagirathi near Devprayag. **d** Landscape configuration at the upper Alaknanda catchment

3 Data and Methodology

3.1 Data Processing

High-resolution digital elevation models are often considered in quantitative landscape evolution studies around the world. In this study, we utilized the Shuttle Radar Topographic Mission (SRTM) digital elevation model (DEM) of 90 m spatial resolution (<http://srtm.csi.cgiar.org>). The DEM was processed in ArcGIS 10.1 to fill data gaps, generating Alaknanda-Bhagirathi catchment and streams, utilizing hydrology tools. We also delineated sub-catchments by carefully selecting all the tributaries that have streams of 4th order while joining the trunk stream. Then we computed relief, slope, and hypsometric integral [mean elevation-min elevation/max elevation- min elevation] for all the sub-catchments.

We plotted longitudinal profiles in MATLAB (<https://www.mathworks.com>) based stream profiler tool (<https://geomorphtools.geology.isu.edu>). Then normalized steepness index (k_{sn}) for the entire stream network was estimated in TopoToolbox (Schwanghart and Kuhn 2010).

Pixel-based TRMM precipitation data (www.geog.ucsb.edu/~bodo/TRMM) was utilized for swath profiling and rainfall- k_{sn} correlation.

3.2 Longitudinal Profile and Steepness-Concavity Analysis

The effect of spatially varying rock uplift rates on the bedrock river profiles can be understood from the steepness index (Howard et al. 1994; Kirby and Whipple 2001). The river profile evolution can be expressed as an equation through the incision modeling of the power-law function of channel gradient and drainage area (Howard and Kerby 1983; Howard 1994; Kirby and Whipple 2001):

$$\frac{dz}{dt} = U(x, t) - K A^m S^n \quad (1)$$

where dz/dt indicates the changes in the bedrock elevation through time, U indicates the rate of bedrock uplift while the base-level is constant, S is the local channel gradient, A is the upstream drainage area and K is the coefficient of erosion. The constants m and n are positive and are closely related to erosion, hydraulic geometry, and hydrology (Howard et al. 1994; Whipple and Tucker 1999). For equilibrium condition, the above equation can be rewritten as:

$$S_c = \left(\frac{U}{K} \right)^{1/n} A^{-\left(\frac{m}{n}\right)} \quad (2)$$

and

$$S = k_s A^{-\theta} \quad (3)$$

where S denotes the slope, k_s is the steepness index and θ indicates the concavity index. Since past decades, several studies have suggested a close relationship between erosion rate and the steepness index. As differential uplift has different erosion rates along the channel, as a proxy, this index can be used to determine the variable uplift of a catchment. Although the steepness index is a good indicator of varying uplift, k_s can significantly be affected by lithological variation (Das 2020). Moreover, departures from the normal concavity ($\theta = 0.5 \pm 0.2$) may indicate tectonic uplift by disrupting the longitudinal profile (Burbank and Anderson 2012). In this study, the k_s values are normalized using a reference concavity (θ) of 0.45 for comparison of the steepness in different reaches, tributaries and sub-tributaries.

4 Neo-Tectonic Movement and Channel Evolution

4.1 Longitudinal Profiles of Bhagirathi-Alaknanda

Figure 4 shows longitudinal profiles of the Bhagirathi and Alaknanda rivers. It can be clearly observed that characterized by the glacier domain, first few kilometers of Alaknanda show a very steep gradient. Later, the river shows a series of knickpoints in between the Himalayan thrusts (STD and MCTs). These thrusts closely match with the knickpoints in Alaknanda (Fig. 4). From the source to the MCT I, the Alaknanda forms the knick zone. After crossing the MCT I, the gradient becomes very low. Compared to the Alaknanda, the Bhagirathi river shows a lesser gradient and fewer knick points. While Alaknanda shows prominent knicks in between MCT I and MCT II (MCT II is also known as Vaikrita thrust), such knicks are not very common in the Bhagirathi. Most of the major steep sections on the longitudinal profile are located above the MCT II.

4.2 Steepness-Concavity Index and Influence of Major Thrusts

In the present study, k_{sn} and θ are calculated for reaches in between major thrusts or distinct steeper topography. The longitudinal profile of Alaknanda is divided into four sections for the steepness concavity analysis. The normalized steepness index (k_{sn}) above STD is 121 ($\theta = 0.23 \pm 0.076$), followed by 792 ($\theta = -0.54 \pm 0.3$) in between STD and MCT II, 446 ($\theta = -17 \pm 40$) between MCT II and MCT I,

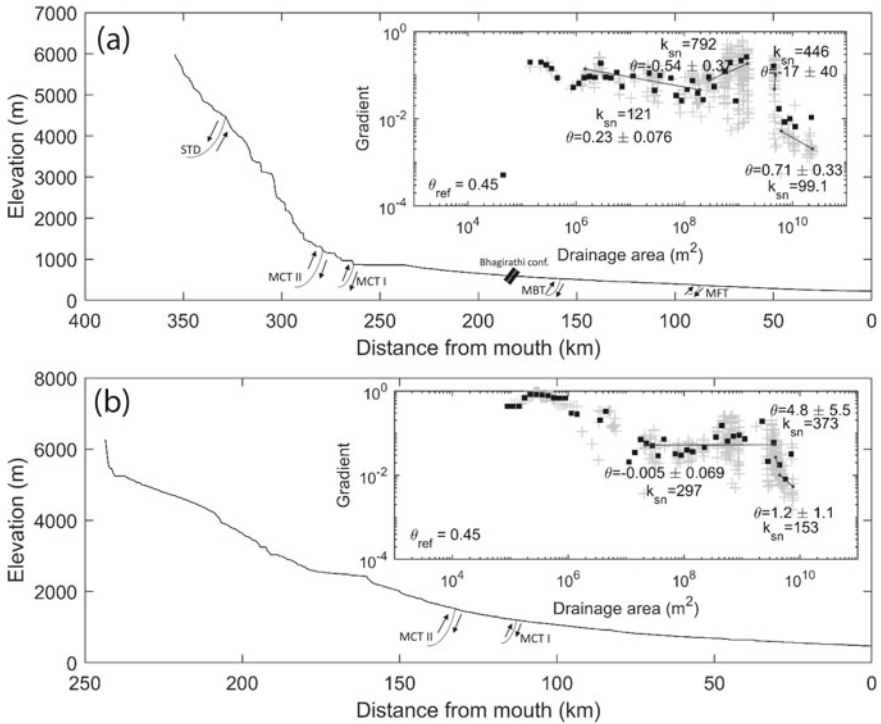


Fig. 4 Longitudinal profiles and the steepness-concavity index in between thrusts and major steep reaches. **a** Alaknanda; **b** Bhagirathi

and 99.1 ($\theta = 0.71 \pm 0.33$) from MCT I to Ganga plain, respectively, from north to south. A careful observation indicates that most of the knickpoints in the study area are distributed between MCT I and STD.

For the Bhagirathi, k_{sn} was calculated for three reaches (a) the irregular elevated, steeper topography in the upper-middle section above MCT II (VT), (b) between MCT II and MCT I and (c) relatively gentle middle-downstream reach. The k_{sn} value in the upper Bhagirathi above MCT II is 297 ($\theta = -0.005 \pm 0.16$), between MCT II and MCT I is 373 ($\theta = 4.8 \pm 5.5$) in, and in the gentler plain section below MCT I until Alaknanda confluence the k_{sn} is 153 ($\theta = 1.2 \pm 1.1$).

Several workers have reported that during the Pleistocene to Holocene periods, major boundary thrusts and faults (e.g. MBT, North Almora Thrust, MCT Alaknanda fault etc.) were active in this region (Sundriyal et al. 2007). Considering this, it is obvious that the geomorphology of this region is highly influenced by the tectonic perturbation by modifying the paleo-landscape. The active landscape has been directed to form some remarkable geomorphic features such as deep incision, changes in river courses and meanders, deformed and uplifted sequential fluvial terraces etc. (Sati et al. 2008) as a result of the recent mountain building process.

Vance et al. (2003) studied the erosion and exhumation rates in the Bhagirathi-Alaknanda catchment using in-situ ^{10}Be cosmogenic dating. In this study, besides longitudinal profile, a k_{sn} map for all the tributaries and sub-tributaries was prepared for the study area (Fig. 5a) for correlating the erosion rates at different thrust regions using the data produced by Vance et al. (2003). A significant positive correlation between k_{sn} and erosion rate is observed (Fig. 6) and therefore, any conclusion drawn from the k_{sn} may be considered as valid. Vance et al. (2003) showed a very

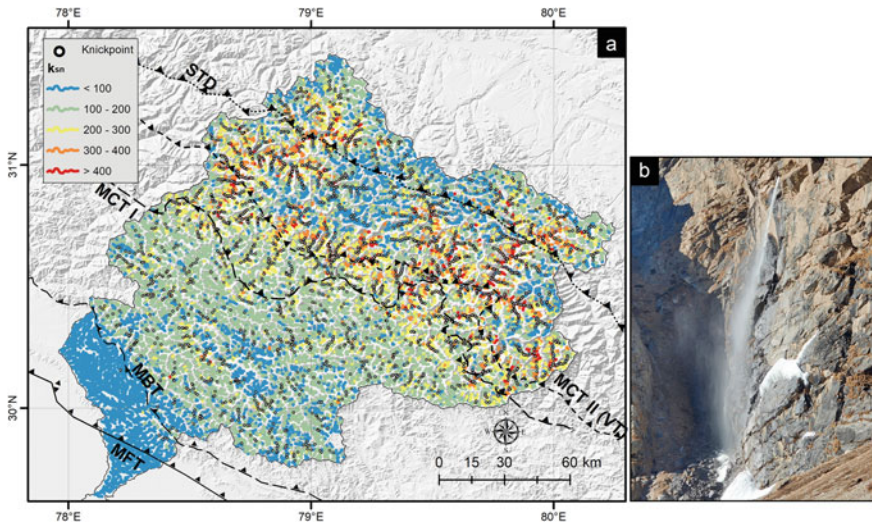
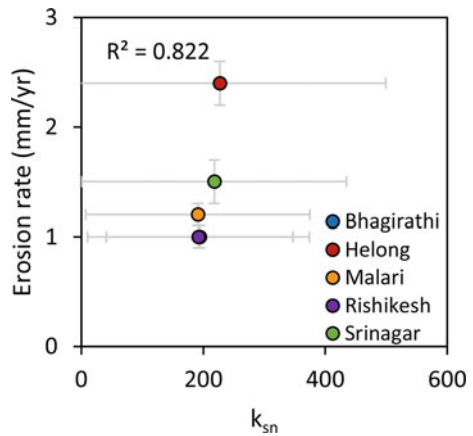


Fig. 5 a Variation of the normalized steepness index (k_{sn}) and knickpoint distribution in the Bhagirathi-Alaknanda catchment. Knickpoints are identified mathematically in MATLAB based Topotoolbox algorithm. The mathematical algorithm identified 2466 knickpoints in the study area. b Vasudhara knickpoint in the upper Alaknanda catchment

Fig. 6 Correlation between normalized steepness index (k_{sn}) and ^{10}Be derived erosion rates at upstream of several locations. ^{10}Be derived erosion rates for the study area are taken from Vance et al. (2003). Note that the data of Bhagirathi and Rishikesh are overlapping on the graph



high erosion rate in upstream of Helong ($2.4 \pm 0.2 \text{ mm yr}^{-1}$), followed by Srinagar ($1.5 \pm 0.2 \text{ mm yr}^{-1}$), Malari ($1.2 \pm 0.1 \text{ mm yr}^{-1}$), Bhagirathi and Rishikesh (both $1.0 \pm 0.1 \text{ mm yr}^{-1}$). This study shows a very consistent values of average k_{sn} in the upstream of Helong ($k_{sn} = 227$), Srinagar ($k_{sn} = 218$), Malari ($k_{sn} = 191$), Bhagirathi ($k_{sn} = 194$) and Rishikesh ($k_{sn} = 192$).

4.3 Estimation of Erosion Rates Between Thrusts

The integrated study of the longitudinal profile, steepness index and concavity index gives good insights into spatial distribution of differential erosion in Bhagirathi-Alaknanda basins. The upstream regions of the Alaknanda-Bhagirathi catchment in between MCTs show deep incisions and steeper gradients compared to the other reaches. Therefore, it may be said that in the study area, differential rock-uplift rate exerts a critical control on the channel gradient and that makes a difference in the steepness and concavity of the channels in different reaches.

Using the linear regression equation derived from the relationship between k_{sn} (this study) and erosion rate (Vance et al. 2003), a further estimation of the average erosion–deposition rates between thrust are calculated by the following equation:

$$\text{Erosion rate} = (0.0314 \times k_{sn}) - 5.0075 \tag{4}$$

while the regression showed $R = 0.91$, and $p \text{ value} = 0.03$.

Table 1 shows that the average k_{sn} value above STD (toward Tibet) is 178 while the derived average erosion rate is 0.58 mm/yr . Although the Tethyan sediment is more erodible than Himalayan crystalline rocks, the dominance of glacial activity over the fluvial process is the main reason behind the lower erosion rate above STD. Most of the landscape in this region is covered by Alpine and Valley glaciers that make a

Table 1 Average normalized steepness index (k_{sn}) and erosion/deposition rates at regions in between major thrusts

Region	Average k_{sn}	Erosion (+) or deposition (–) rate (mm/yr)
Above STD	178	0.58
Between MCT II and STD	237	2.43
Between MCT I and MCT II	251	2.87
Between MBT and MCT I	146	–0.42
Between MFT and MBT	30	–4.07
Ganga plain	13	–4.60

thick veneer on the rocky substrate and prevent intensive erosion. Consequently, the region between MCT I and II show the maximum estimated rate of erosion ($k_{sn} = 251$; erosion rate = 2.87 mm/yr). This region is found to have differential exhumation rates through geological past with a rapid exhumation of garnet rock as high as 9 mm/yr reported after reactivation of MCT during Miocene (~8 Myr) (Harrison et al. 1997; Catlos et al. 2001; Vance et al. 2003). Several studies suggest that in tectonically active landscape, differential k_{sn} values between faults indicate differential uplift (Kirby and Whipple 2001). Tyagi et al. (2009) suggested that the MCT region of the Alaknanda falls under a higher rate of uplift. Hence, based on results from this study, it can be said that the higher erosion rate between MCT I and MCT II may be a result of a higher uplift rate which is reflected by a higher frequency of landslides (Sarkar et al. 2015). Also, the MCT region shows high relief topography compared to the region above STD, which could be possibly another reason behind active incision and higher erosion rate. However, the negative values southwards of MBT (Table 1) indicate dominant depositional regime although, the present inferences are purely based on a statistical correlation between the erosion rate and k_{sn} , demanding further validation. Based on the above information, the average rates of deposition between MBT-MCT I, MFT-MBT and on the frontal plain are estimated as 0.42, 4.07 and 4.59 mm/yr, respectively.

4.4 Correlation of Landscape Variables and Rainfall with k_{sn}

Correlation between geomorphic parameters that are related to erosion (e.g. elevation, relief, slope, hypsometry etc.), rainfall, and lithology as independent factors and the normalized steepness index (k_{sn}) as dependent factor provides critical quantitative information about the potential control of the erosion in a given area (Abrahami et al. 2016). Therefore, although our study mainly focused on understanding differential uplift with respect to varying uplift rates in between major thrusts, in addition, we correlated major potentially controlling factors of the varying erosion rate in the Alaknanda-Bhagirathi catchment (Fig. 7). Among five variables (mean elevation, relief, slope, hypsometric integral, and rainfall) only relief is found to have a significant relation with k_{sn} ($R = 0.698$, $\alpha = 0.05$). It implies that, in the Alaknanda-Bhagirathi catchment, regions with a great elevation range experience greater erosion. Moreover, all these high relief catchments were found to have fluvially dominant processes contributing a large area between MCT I and II.

The evolution of the Indian Summer Monsoon in the Himalayan region is hand in hand with the evolution of mountain building processes which are marked by the thrust reactivations in this region. The absence of any correlation between the spatial distribution of precipitation and k_{sn} indicates the landscape processes and erosion rates are more controlled by tectonics than climate. Abrahami et al. (2016) showed a similar observation in Sikkim Himalayas, where they concluded that while erosion rates are highly correlated to k_{sn} and primarily controlled by tectonic uplift, precipitation only has a secondary control.

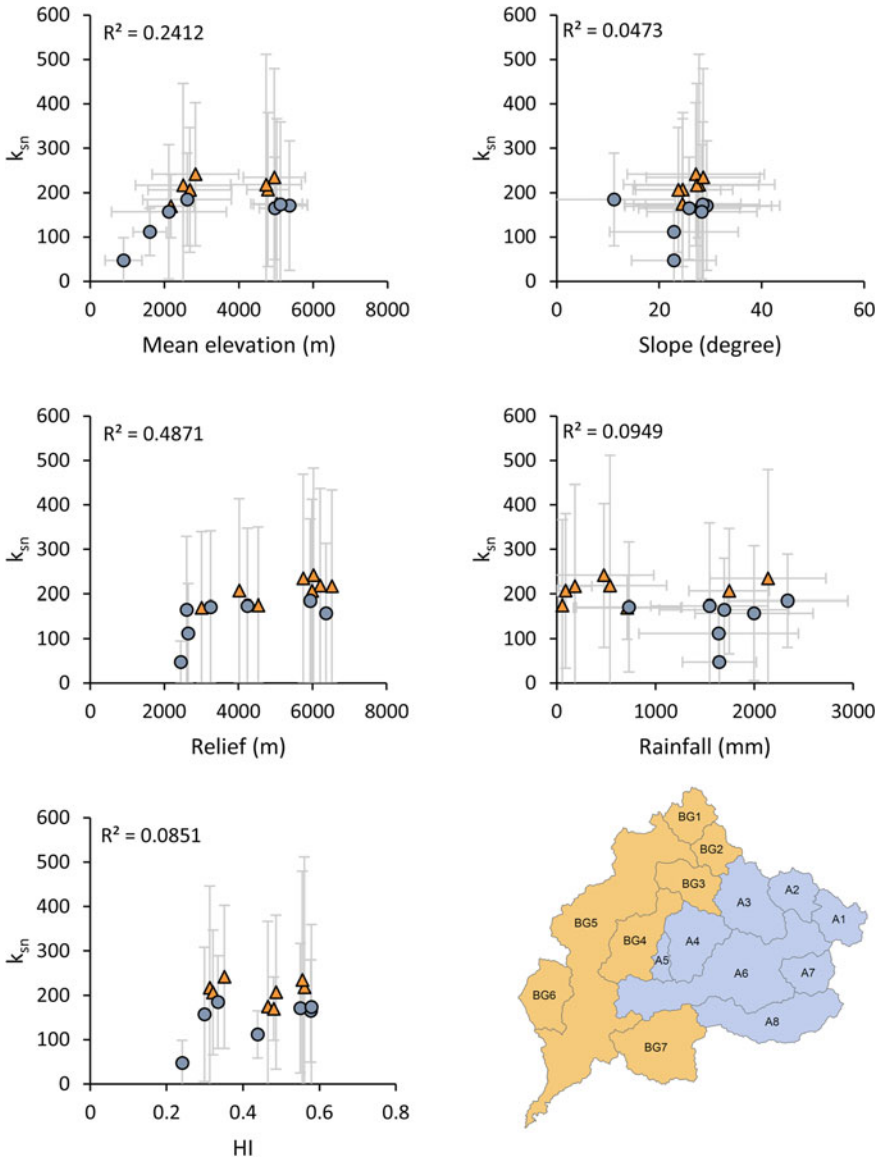


Fig. 7 Correlation between major driving factors with k_{sn} . Blue and orange dots indicate subcatchments in Alaknanda and Bhagirathi-Ganga respectively

In understanding the complex nature of coupled tectonic and climatic influence on the evolution of post-orogenic mountains, rock uplift, and erosion; k_{sn} have been extensively considered as a proxy of erosion rate because of its strong correlation with in-situ based erosion rate data (e.g. Abrahami et al. 2016; Dey et al. 2016; Scherler et al. 2017; Nennewitz et al. 2018; Adams et al. 2020). The k_{sn} data is proven to be efficient in comprehending such external perturbations on the landscape dynamics and varying erosion rates in a systematic way. Based on the outcomes of our study and the previously published studies, this method can be considered as one of the simplest approaches that may be applicable in other regions in the Himalayas to understand the impact of tectonics and monsoon climate on topographic evolution even for the regions where in-situ based erosion rate data are unavailable.

5 Conclusion

River longitudinal profiles and distribution of normalized steepness index (k_{sn}) provide significant insight into the landscape evolution and erosion potential of a region. Our study demonstrates a systematic analysis of river longitudinal profiles and k_{sn} to comprehend the role of varying uplift rate, geomorphic indices and monsoon rainfall in differential erosion rates in between major thrusts in the Alaknanda-Bhagirathi catchment. A significant correlation between ^{10}Be derived erosion rate and k_{sn} indicated high rate of erosion (2.87 mm/yr) between MCT I and II. Fluvial processes may have a dominant role in erosion as the maximum erosion rate is found between MCT I and II where the region is under transition from the glacial to the fluvial regime with intense headward erosion. Though topographic relief has significant control on erosion rate in this region, because of no correlation between rainfall and k_{sn} , we conclude that differential tectonic uplift is the main driving factor in topographic evolution while rainfall exerts a secondary control.

Acknowledgements S.D. wishes to thank UGC-India for financial support. The authors wish to thank Heads, Department of Geography and Geology, Savitribai Phule Pune University for providing necessary facilities to carry out this study. Constructive comments from two anonymous reviewers improved the final chapter significantly. We thank the editors of this book for their generous helps and supports during the entire editorial process.

References

- Abrahami R, Beek PVD, Huyghe P, Hardwick E, Carcaillet J (2016) Decoupling of long-term exhumation and short-term erosion rates in the Sikkim Himalayas. *Earth Planetary Sci Lett* 433:76–88
- Adams BA, Whipple KX, Forte AM, Heimsath AM, Hodges KV (2020) Climate controls on erosion in tectonically active landscapes. *Sci Adv* 6:eaa3166

- Bhakuni SS, Luirei K, Kothyari GC, Imsong W (2017) Transverse tectonic structural elements across Himalayan mountain front, eastern Arunachal Himalayas, India: implication of superposed landform development on analysis of neotectonics. *Geomorphology* 282:176–194
- Bookhagen B, Burbank DW (2006) Topography, relief and TRMM-derived rainfall variation along the Himalayas. *Geophys Res Lett* 35:L08405
- Burbank DW, Anderson RS (2012) *Tectonic geomorphology*. Blackwell Science, Oxford
- Catlos EJ, Harrison TM, Kohn MJ, Grove M, Ryerson FJ, Manning CE, Upreti BN (2001) Geochronologic and thermobarometric constraints on the evolution of the Main Central Thrust, central Nepal Himalayas. *J Geophys Res* 106:16177–16204
- Das S (2020) Koyana-Warna shallow seismic region, India: Is there any geomorphic expression of active tectonics? *J Geol Soc India* 96:217–231
- Dewey J, Bruke K (1973) Tibetan, Variscan and Precambrian basement reactivation: products of continental collision. *J Geol* 81:683–692
- Dey S, Thiede RC, Schildgen TF, Wittmann H, Bookhagen B, Scherler D, Strecker MR (2016) Holocene internal shortening within the northwest Sub-Himalayas: out-of-sequence faulting of the Jwalamukhi Thrust, India. *Tectonics* 35:2677–2697
- Dimri AP, Niyogi D, Barros AP, Ridley J, Mohanty UC, Yasunari T, Sikka DR (2015) Western disturbances: a review. *Rev Geophys* 53:225–246
- Fasullo J, Webster PJ (2003) A hydrological definition of Indian monsoon onset and withdrawal. *J Clim* 16:3200–3211
- Harrison TM, Ryerson FJ, Le Fort P, Yin A, Lovera OM, Catlos EJ (1997) A late Miocene-Pliocene origin for the central Himalayan inverted metamorphism, Earth Planet. Sci Lett 146:E1–E7
- Howard AD (1994) A detachment-limited model of drainage basin evolution. *Water Resour Res* 30:2261–2285
- Howard AD, Kerby G (1983) Channel changes in badlands. *Geol Soc Am Bull* 94:739–752
- Howard AD, Seidl MA, Dietrich WE (1994) Modeling fluvial erosion on regional to continental scales. *J Geophys Res* 99:13971–13986
- Kirby E, Whipple K (2001) Quantifying differential rock-uplift rates via stream profile analysis. *Geology* 29:415–418
- Kothyari GC, Luirei K (2016) Late quaternary tectonic landforms and fluvial aggradation in the Saryu River Valley: Central Kumaun Himalayas. *Geomorphology* 268:159–176
- Nennewitz M, Thiede RC, Bookhagen B (2018) Fault activity, tectonic segmentation and deformation pattern of the western Himalayas on Ma timescale inferred from landscape morphology. *Lithosphere* 10:632–640
- Patriat P, Achache J (1984) India-Eurasia collision chronology has implications for crustal shortening and driving mechanism of plates. *Nature* 311:615–621
- Pichon XL, Fournier M, Jolivet L (1992) Kinematics, topography, shortening, and extrusion in the India-Eurasia collision. *Tectonics* 11:1085–1098
- Rana N, Singh S, Sundriyal YP, Rawat GS, Juyal N (2016) Interpreting the geomorphometric indices for neotectonic implications: an example of Alaknanda valley, Garhwal Himalayas, India. *J Earth Sys Sci* 125:841–854
- Ray Y, Srivastava P (2010) Widespread aggradation in the mountainous catchment of the Alaknanda-Ganga river systems: timescales and implications to Hinterland-foreland relationships. *Quatern Sci Rev* 29:2238–2260
- Rees HG, Collins DN (2006) Regional differences in response of flow in glacier-fed Himalayan Rivers to climatic warming. *Hydrol Process* 20:2157–2169
- Sarkar S, Kanungo DP, Sharma S (2015) Landslide hazard assessment in the upper Alaknanda valley of Indian Himalayas. *Geomat Nat Hazard Risk* 6:308–325
- Sati SP, Rana N, Kumar D, Reddy DV, Sundriyal YP (2008) Pull-apart origin of wider segments of the Alaknanda Basin Uttarakhand Himalayas, India. *Himal Geol* 29:89–90
- Scherler D, DiBiase RA, Fisher GB, Avouac J (2017) Testing monsoonal controls on bedrock river incision in the Himalayas and Eastern Tibet with a stochastic-threshold stream power model. *J Geophys Res Earth Surf* 122:1389–1429

- Schwanghart W, Kuhn NJ (2010) TopoToolbox: a set of Matlab functions for topographic analysis. *Environ Model Softw* 25:770–781
- Seeber L, Armbruster JG, Quittmeyer RC (1981) Seismicity and continental subduction in the Himalayan Arc. In: Gupta HK, Delany FM (eds) *Zagros, Hindukush, Himalayas, geodynamic evolution*. Geodynamic series, vol 3. American Geophysical Union, Washington, pp 215–242
- Sharma G, Champati ray PK, Mohanty S (2018) Morphotectonic analysis and GNSS observations for assessment of relative tectonic activity in Alaknanda basin of Garhwal Himalayas, India. *Geomorphology* 301:108–120
- Singh S (2018). Alaknanda-Bhagirathi river system. https://doi.org/10.1007/978-981-10-2984-4_8
- Singh M, Singh IB, Muller G (2007) Sediment characteristics and transportation dynamics of the Ganga River. *Geomorphology* 86:144–175
- Singh DS, Gupta AK, Sangode SJ, Clemens SC, Prakasam M, Srivastava P, Prajapati SK (2015) Multiproxy record of monsoon variability from the Ganga Plain during 400–1200 A.D. *Quatern Int* 371:157–163
- Sinha S, Sinha R (2016) Geomorph evolution of Dehra Dun, NW Himalayas: tectonics and climate coupling. *Geomorphology* 266:20–32
- Sundriyal YP, Jayant T, Sati SP, Rawat GS, Srivastava P (2007) Landslide dammed lakes in the Alaknanda basin, Lesser Himalayas: causes and implications. *Curr Sci* 93(4):568–574
- Thiede RC, Arrowsmith JR, Bookhagen B, McWilliams MO, Sobel ER, Strecker MR (2005) From tectonically to erosionally controlled development of the Himalayan orogen. *Geology* 33:689–692
- Tyagi AK, Chaudhary S, Rana N, Sati SP, Juyal N (2009) Identifying areas of differential uplift using steepness index in the Alaknanda basin, Garhwal Himalayas, Uttarakhand. *Curr Sci* 97:1473–1477
- Valdiya KS (1988) Tectonics and evolution of the central sector of the Himalayas. *Phil Trans R Soc Lond A* 326:151–175
- Vance D, Bickle M, Ivy-Ochs S, Kubik PW (2003) Erosion and exhumation in the Himalayas from cosmogenic isotope inventories of river sediments. *Earth Planet Sci Lett* 206:273–288
- Wasson RJ, Juyal N, Jaiswal M, Culloch M, Sarin MM, Jain V, Srivastava P, Singhvi AK (2008) The mountain-lowland debate: deforestation and sediment transport in the Upper Ganges catchment. *J Environ Manage* 88:53–61
- Whipple KX, Tucker GE (1999) Dynamics of the stream-power river incision model: implications for height limits of mountain ranges, landscape response timescales, and research needs. *J Geophys Res* 104:17661–17674
- Whitehouse IE (1990) Geomorphology of the Himalayas: a climate-tectonic framework. *NZ Geogr* 46:75–85